

Communication

# Fabrication of Carbon Aerogels Derived from Metal-Organic Frameworks/Carbon Nanotubes/Cotton Composites as an Efficient Sorbent for Sustainable Oil–Water Separation

Yinyu Sun , Zhongcheng Ke \*, Caiyun Shen, Ruikang Sun, Qing Wei, Zihan Yin and Wei Yang

School of Chemistry and Chemical Engineering, Huangshan University, Huangshan 245021, China; yysun\_hsu@163.com (Y.S.); ascy8843@163.com (C.S.); sunruikangjnu@163.com (R.S.); wq19105591009@163.com (Q.W.); yzh20030201@163.com (Z.Y.); myxhjsn996320687@163.com (W.Y.)

\* Correspondence: xiaoke1020@126.com; Tel.: +86-139-5599-7920

**Abstract:** Due to the continuous occurrence of water pollution problems, practical separation methods for oil–water mixtures have attracted more and more attention. To date, different kinds of materials have been developed with good hydrophobic properties and strong separation ability. Carbon aerogels, as a promising ideal adsorbent for dealing with oil-spill accidents, have received extensive attention. In this work, zeolitic imidazolate frameworks (ZIFs), nanoparticles, and carbon nanotubes (CNTs) in the three-dimensional (3D) interconnected network structure of cotton balls (CBs) were successfully prepared by a simple and scalable process. The as-prepared carbonized CBs with carbonized ZIF-8 and CNTs (CZIF-8/CNTs/CCBs) were characterized. The oil–water separation performance of the composite was also measured. The results show that the ZIF-8 clusters intercalated with abundant CNTs are fully loaded into the porous structure of the CBs after the in situ synthesis process. Additionally, ZIF-8/CNTs/CBs was carbonized in nitrogen, leading to the formation of CZIF-8/CNTs/CCBs. The prepared material possesses excellent hydrophobicity with a water contact angle of 152.7°, showing good absorption capacities  $Q_1$  in the range of 48 to 84 times its original weight for oil and organic liquids. In addition, CZIF-8/CNTs/CCBs exhibits good recyclability in the absorption–distillation test. In summary, this study proposes a novel and simple method for the preparation of a superhydrophobic material that could have wide application in the separation of oil–water mixtures.

**Keywords:** zeolitic imidazolate frameworks; carbon nanotubes; cotton balls; oil–water separation



**Citation:** Sun, Y.; Ke, Z.; Shen, C.; Sun, R.; Wei, Q.; Yin, Z.; Yang, W. Fabrication of Carbon Aerogels Derived from Metal-Organic Frameworks/Carbon Nanotubes/Cotton Composites as an Efficient Sorbent for Sustainable Oil–Water Separation. *Appl. Sci.* **2022**, *12*, 7285. <https://doi.org/10.3390/app12147285>

Academic Editors: Mohammad Mahmudur Rahman, Dibyendu Sarkar, Rupali Datta and Prafulla Kumar Sahoo

Received: 21 June 2022

Accepted: 19 July 2022

Published: 20 July 2022

**Publisher's Note:** MDPI stays neutral with regard to jurisdictional claims in published maps and institutional affiliations.



**Copyright:** © 2022 by the authors. Licensee MDPI, Basel, Switzerland. This article is an open access article distributed under the terms and conditions of the Creative Commons Attribution (CC BY) license (<https://creativecommons.org/licenses/by/4.0/>).

## 1. Introduction

The frequent occurrences of oil pollution issues have become more and more alarming. It is very important to find effective strategies to solve the aforementioned issues [1–5]. Oil–water separation materials with a porous structure and a superhydrophobic surface, such as sponges [6–9], foams [10–14], carbon aerogels [15–17], and meshes [18–20], have been widely studied due to their excellent water repellency and good oil–water separation capacity. The preparation of these superhydrophobic materials is based on changing the chemical composition or the microscopic structure [21–24]. In nature, biomass materials possess many exceptional biological properties by virtue of their unique structures, and these materials are gaining significant attention [25,26]. Cotton, a typical environmentally friendly biomass material, contains abundant cellulose fibers with hydrophilic surface hydroxyl groups and a three-dimensional (3D) network structure [27–29]. The modification of cotton to produce superhydrophobic materials for the separation of water and oil has been widely investigated in recent decades [30,31]. Nevertheless, most of the preparation methods have some limitations such as a cumbersome preparation process, expensive reagents, or low oil sorption capacity. Hence, it is highly desirable to develop a facile and green method for synthesizing highly hydrophobic composites derived from cotton with

high separation capacity and low material costs, for dealing with substandard oil–water mixtures and offshore crude oil leaks.

In this study, carbon aerogels were prepared by anchoring zeolitic imidazolate frameworks (ZIFs), nanoparticles, and carbon nanotubes (CNTs) on the surface of cotton balls (CBs), followed by carbonization. The carbonized ZIF-8 and CNTs on carbonized CBs (CZIF-8/CNTs/CCBs) were examined by field emission scanning electron microscopy (FE-SEM), Fourier transform infrared spectroscopy (FTIR), X-ray photoelectron spectroscopy (XPS), energy-dispersive X-ray spectrometry (EDS), and X-ray diffraction (XRD). Furthermore, the oil–water separation performance and the reusability of the samples were also examined. The results show that the material prepared in this study has good prospects for application in the field of oil–water separation.

## 2. Materials and Methods

### 2.1. Materials

Zinc nitrate hexahydrate, 2-methylimidazole, methanol, and ethanol were supplied by Sinopharm Chemical Reagent Co., Ltd. (Shanghai, China). Industrial multiwalled carbon nanotubes were obtained from Macklin Biochemical Co., Ltd. (Shanghai, China). The commercial CBs were washed with ethanol for 1 h and dried at 80 °C for 5 h.

### 2.2. Preparation of CZIF-8/CNTs/CCBs

In a typical procedure, ZIF-8 and CNTs coated on CBs were successfully prepared by an in situ synthesis method. A total of 0.8 g of 2-methylimidazole was dissolved in methanol (8 mL), denoted as solution A. CBs were dipped into solution A, followed by stirring for about 1 h at room temperature. Then, 0.06 g of CNTs was dipped into the above solution under stirring for 2 h. Subsequently, 8 mL of methanol containing zinc nitrate hexahydrate (0.4 g) was added into the prepared mixture, stirring for 12 h. The as-obtained ZIF-8/CNTs/CBs was washed with deionized water and dried at 80 °C for 5 h. CZIF-8/CNTs/CCBs was prepared by carbonizing the homologous precursors in nitrogen for 2 h at 600 °C.

### 2.3. Physical Characterization

The surface microstructure of the samples was investigated using FE-SEM (Gemini 500, Zeiss, Oberkochen, Germany) and TEM (Tecnai G<sup>2</sup> F20, FEI, Ames, IA, USA). The surface chemical composition was characterized using EDS (X-Max<sup>N</sup> 80, Oxford, UK), FTIR (Spirit-T, Shimadzu, Chiyoda-ku, Tokyo, Japan), and XPS (ESCALAB 250Xi, Thermo Fisher, Waltham, MA, USA). X-ray diffraction patterns were recorded using an XRD apparatus equipped with a Cu K $\alpha$  radiation source (D8 Advance, Bruker, Karlsruhe, Germany). The water contact angles of the samples were measured using a contact angle meter (DSA100, KRÜSS, Hamburg, Germany).

### 2.4. Oil–Water Separation Test

To evaluate the practical applications of the samples, the oil–water separation capacity was measured. In a typical test, the sample was first weighed and subsequently immersed in various organic solvents and oils for 1 min. Then, the sample was taken out for immediate weight measurement. The adsorption capacity of the sample was evaluated by  $Q_1$  and  $Q_2$ . The adsorption capacity  $Q_1$  was calculated through the following equation:  $Q_1 = (W_2 - W_1)/W_1$ , where  $W_1$  and  $W_2$  are the masses of the sample before and after absorption, respectively. The adsorption capacity  $Q_2$  was assessed according to the following equation:  $Q_2 = (W_2 - W_0)/W_0$ , where  $W_0$  and  $W_2$  are the masses of the raw CBs and the sample, respectively. In the absorption–distillation test, n-heptane was sorbed by CZIF-8/CNTs/CCBs. Then, the used material was evaporated at a temperature around the boiling point (100 °C) of n-heptane. All the tests were performed under the same conditions.

### 3. Results and Discussion

The preparation process for CZIF-8/CNTs/CCBs involved three steps, as illustrated in the schematic diagram in Figure 1. Firstly, the 3D interconnected network structure of the CBs was fully wetted by the solution of 2-methylimidazole, which can result in active sites on the surface of the CBs for ZIF-8 growth. In this process, CBs were not only used as the support to adsorb the 2-methylimidazole but also acted as the porous structure for the loading of ZIF-8 and CNTs in the next step. Secondly, after adding a certain amount of CNTs and the solution of zinc nitrate, ZIF-8/CNTs/CBs was successfully prepared based on an in situ synthesis method, producing a color change from white to black. The addition of CNTs can not only enhance the cross-linking action of ZIF-8 but can also effectively improve the adsorption performance during the oil–water separation process. In the meantime, the prepared ZIF-8 was tightly adhered in the 3D interconnected network structure of the CBs, also improving the adsorption capacity due to its porous structure. Finally, ZIF-8/CNTs/CBs was carbonized in nitrogen at 600 °C, leading to the formation of CZIF-8/CNTs/CCBs with a superhydrophobic surface.

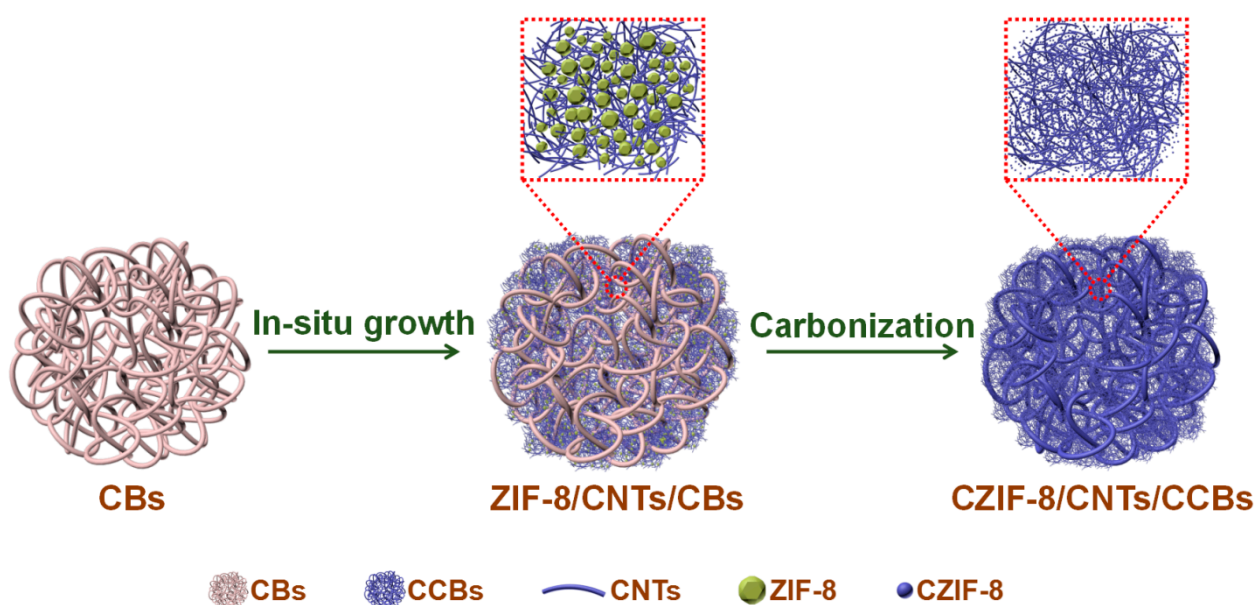


**Figure 1.** Schematic illustration of the preparation of CZIF-8/CNTs/CCBs.

The surface microstructure of the samples was observed using FE-SEM images of different magnifications and TEM images. As depicted in Figure 2a,d, the pristine CBs exhibit a 3D interconnected network structure and a relatively smooth surface. After the in situ synthesis process, ZIF-8 and CNTs are fully loaded into the porous structure of the CBs (Figure 2b). The ZIF-8 clusters are composed of ZIF-8 nanoparticles intercalated with abundant CNTs (Figure 2e), which is consistent with the TEM result (Figure 3a). As shown in Figure 2c,f, the ZIF-8 clusters disappear from the surface of the as-synthesized CZIF-8/CNTs/CCBs. The TEM image (Figure 3b) clearly shows that the ZIF-8 clusters are decomposed into ZIF-8 nanoparticles after carbonization.

XPS, EDS, and FTIR were used to investigate the surface chemical composition of the samples. The XPS results in Figure 4a confirm the existence of the elements C (284.8 eV), N (399.9 eV), O (532.8 eV), and Zn (1022.3 eV) in the ZIF-8/CNTs/CBs and CZIF-8/CNTs/CCBs. It is worth noting that the proportion of Zn on the surface of CZIF-8/CNTs/CCBs is clearly higher than for ZIF-8/CNTs/CBs. As can be seen from the data in Figure 4b, the XPS spectra for each element of the ZIFs/CNTs/CBs were obtained and fitted. The C 1s spectrum can be divided into four peaks at 284.5, 284.8, 285.4, and 286.6 eV, corresponding to C–C ( $sp^2$ ), C–C ( $sp^3$ ), C–OH, and C–N, respectively. The N 1s spectrum of ZIF-8/CNTs/CBs reveals three peaks located at 399.5, 400.0, and 401.0 eV,

ascribed to pyridinic N, pyrrolic N, and pyridine N oxide, respectively. The O 1s spectrum of ZIF-8/CNTs/CBs shows three peaks, corresponding to carboxyl C=O bonds at 532.2, and 532.8 eV and hydroxyl oxygen at 533.6 eV [32,33]. The Zn 2p<sup>3</sup> spectrum of ZIF-8/CNTs/CBs contains two individual component peaks at 1022.2 and 1045.3 eV, assigned to the Zn 2p<sup>3/2</sup> and Zn 2p<sup>1/2</sup> electronic states, respectively. This result confirms the presence of zinc oxide, which is consistent with previous work [34]. The EDS elemental mappings shown in Figure 5a reveal that the main elements present are C and O on the surface of the CBs. After the in situ synthesis process, the elements N and Zn were detected on the surface of ZIF-8/CNTs/CBs, which corresponds to the XPS results (Figure 4a). In addition, the EDS result for CZIF-8/CNTs/CCBs reveals that the relative content of Zn showed a marked increase (Figure 4a,b). These results demonstrate that ZIF-8 particles are not only homogeneously deposited but are also abundant on the substrate. FTIR spectra were acquired to further confirm the composition of the CBs, ZIF-8/CNTs/CBs, and CZIF-8/CNTs/CCBs. As can be seen in Figure 6a, the strong broad absorption band at 3400 cm<sup>-1</sup> was assigned to the abundant -OH group on the surface of the CBs. After modification with ZIF-8 and CNTs, a series of absorption bands in the range of 550–1600 cm<sup>-1</sup> were found in ZIF-8/CNTs/CBs, probably caused by the imidazole ring [32]. In particular, the absorption bands at 425 and 1715 cm<sup>-1</sup> are ascribed to the Zn–N stretching vibration band and the C=N stretching vibration band, respectively, which is consistent with earlier reports [35,36].

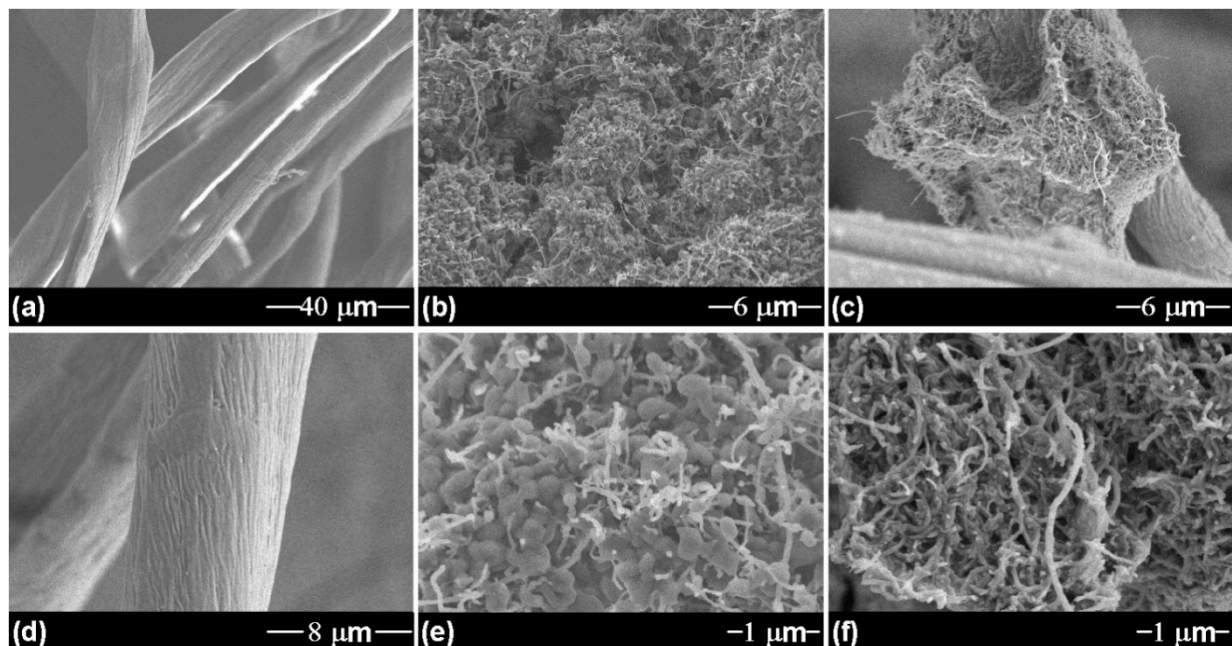


**Figure 2.** FE-SEM images of CBs (a,d), ZIF-8/CNTs/CBs (b,e), and CZIF-8/CNTs/CCBs (c,f).

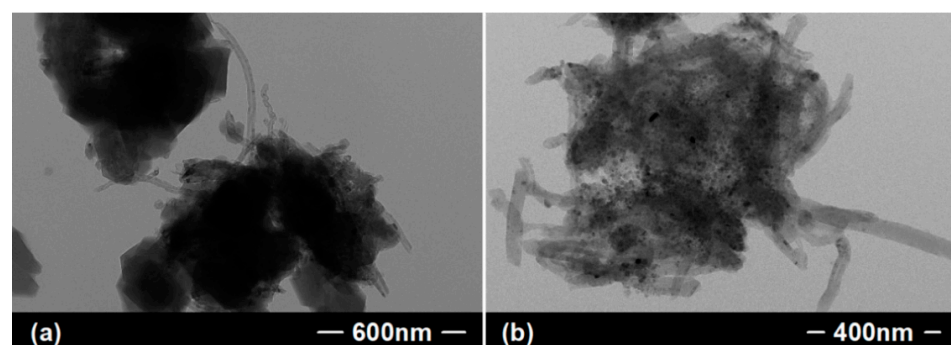


**Figure 3.** TEM images of ZIF-8/CNTs (a) and CZIF-8/CNTs (b).

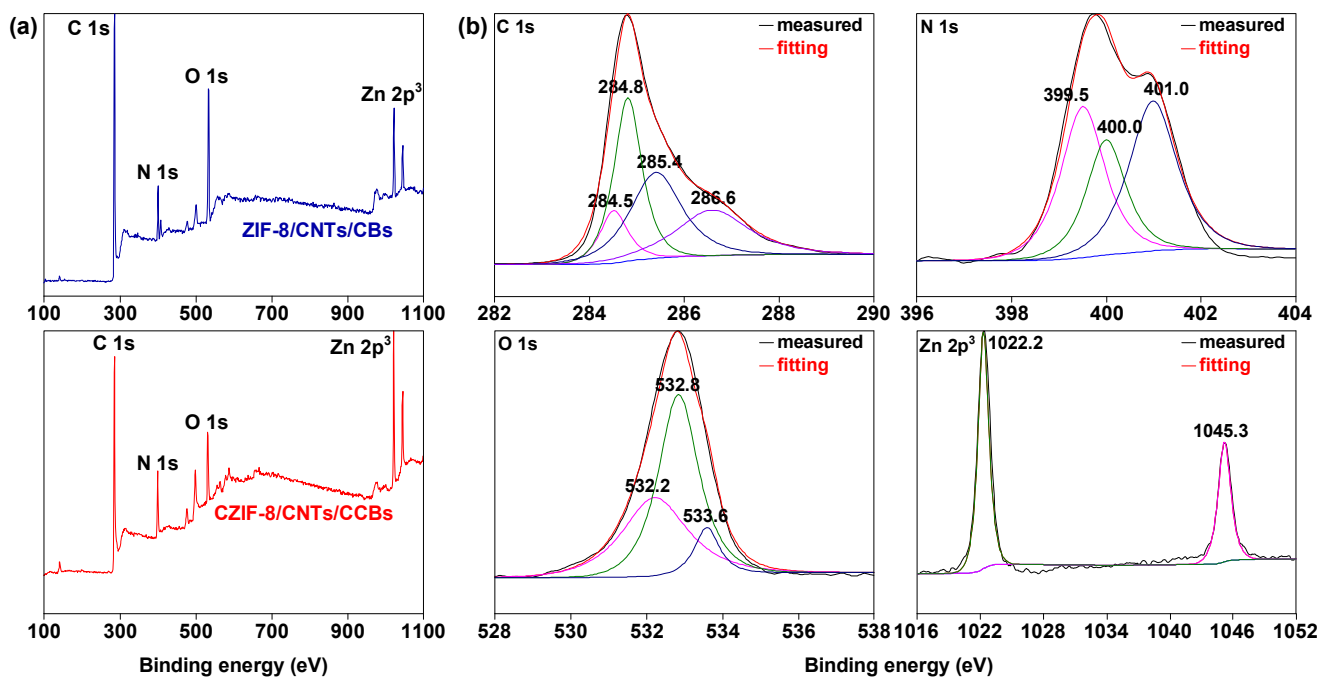


**Figure 4.** (a) XPS survey spectra of ZIF-8/CNTs/CBs and C ZIF-8/CNTs/CCBs. (b) C 1s, N 1s, O 1s, and Zn 2p<sup>3</sup> spectra of ZIF-8/CNTs/CBs.

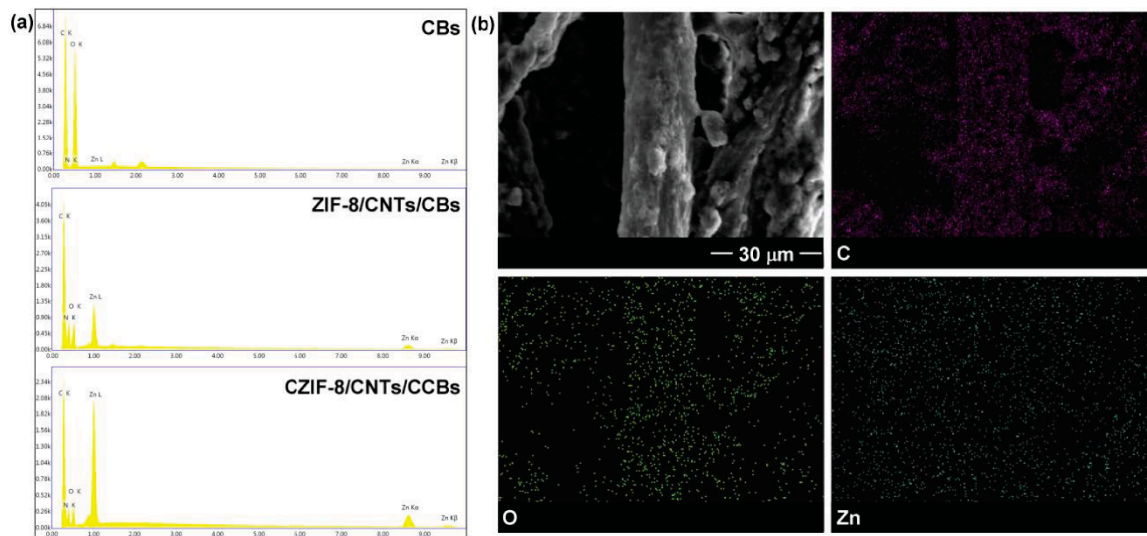


**Figure 5.** (a) Images of CBs, ZIF-8/CNTs/CBs, and CZIF-8/CNTs/CCBs EDS elemental analysis spectra. (b) Images of CZIF-8/CNTs/CCBs in EDS elemental mappings.

The crystalline structures of CBs, ZIF-8/CNTs/CBs, and CZIF-8/CNTs/CCBs were investigated using XRD patterns (Figure 6b). It can be seen that there are three typical diffraction peaks at 14.8°, 16.5°, and 22.9°, which were assigned to the (1–10), (110), and (200) lattice planes of cellulose in the CBs, respectively [37]. The XRD pattern of ZIF-8/CNTs/CBs shows six characteristic peaks at 7.3°, 10.4°, 12.9°, 14.7°, 16.4°, and 18.2°, which can be ascribed to the (011), (002), (112), (022), (013), and (222) lattice planes of ZIF-8, respectively [33]. Moreover, the XRD pattern of CZIF-8/CNTs/CCBs possesses only one weak and broad diffraction peak at 26.1°, corresponding to the (002) lattice plane of the graphite-structure crystallites of CCBs [38]. These XRD results further verify the successful preparation of ZIF-8 on the surface of the CBs.

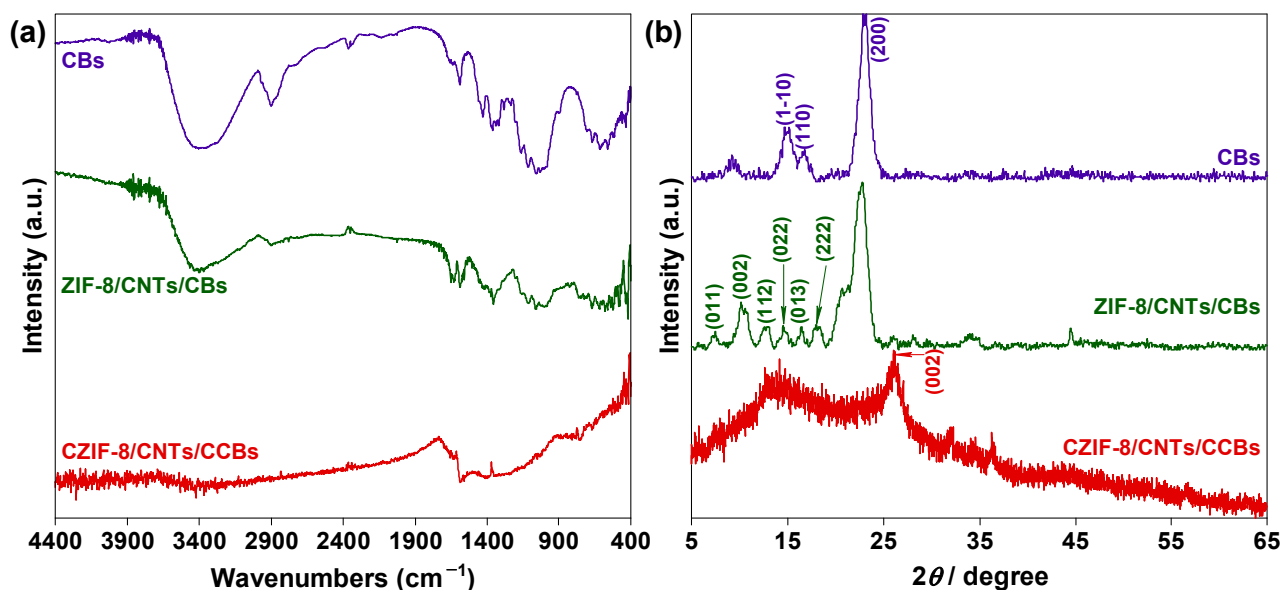


**Figure 6.** (a) FTIR spectra of CBs, ZIF-8/CNTs/CBs, and CZIF-8/CNTs/CCBs. (b) XRD patterns for CBs, ZIF-8/CNTs/CBs, and CZIF-8/CNTs/CCBs.

Figure 7a–c shows the water contact angles of CBs, ZIF-8/CNTs/CBs, and CZIF-8/CNTs/CCBs. CBs and ZIF-8/CNTs/CBs show good hydrophilicity, due to the existence of a hydrophilic group. After carbonization, CZIF-8/CNTs/CCBs possessed a superhydrophobic surface with a water contact angle of 152.7°. Interestingly, the water droplet descended and contacted with the surface of CZIF-8/CNTs/CCBs. However, as the water droplet continued to rise, the water droplet and the surface of the CZIF-8/CNTs/CCBs gradually separated, suggesting that the sample had an ultra-low contact-angle lag (Figure 7d). As shown in Figure 8, the absorption capability of the sample was evaluated. CZIF-8/CNTs/CCBs can quickly and completely absorb dichloromethane dyed by Oil Red O from the bottom of the water (Figure 8a). Furthermore, when CZIF-8/CNTs/CCBs contacted n-hexane dyed by Oil Red O on water, it absorbed the n-hexane in seconds (Figure 8b). These results suggest that this material has excellent oleophilic and hydrophobic properties. The oil–water separation performance of the samples was evaluated by measuring the absorption capacities for various oils and organic liquids (Figure 9a,b). CZIF-8/CNTs/CCBs showed absorption capacities  $Q_1$  in the range of 48 to 84 times its original weight for oil and organic liquids. The absorption capacities  $Q_1$  of CCBs were slightly higher than those of CZIF-8/CNTs/CCBs for most of the oils and organic liquids. However, it is worth noting that the absorption capacity  $Q_2$  of CZIF-8/CNTs/CCBs was much higher than that of CCBs. The possible reason for this result is that CCBs become lighter and smaller after carbonization of the CBs. Although the absorption capacity  $Q_1$  of CCBs for oil and organic liquids is relatively higher, the absorption capacity  $Q_2$  is low on account of the low actual adsorption amount. Meanwhile, ZIF-8 and CNTs were loaded into the 3D interconnected network structure of CBs, and the mass of CZIF-8/CNTs/CCBs was relatively high. Therefore, the value of the absorption capacity  $Q_1$  was lower than that of CCBs. However, the actual adsorption amount of CZIF-8/CNTs/CCBs was much higher, due to the porous structure with large volume and the loading of CZIF-8 and CNTs, resulting in a higher absorption capacity  $Q_2$  value. Therefore, the loading of ZIF-8 and CNTs plays a critical role in improving the adsorption performance of CZIF-8/CNTs/CCBs. As shown in Table 1, the absorption capacity of CZIF-8/CNTs/CCBs is higher than that of various previously reported sorbent materials [31,39–45]. Although the sample shows lower absorption capacity than the reported materials [46–48], the precursor material is cheaper, and the preparation method is simpler. To investigate the recyclability of the sample, the absorption–distillation test was repeated up to nine times. As displayed in

Figure 9c, CZIF-8/CNTs/CCBs retained its high absorption capacity for n-heptane after nine cycles, indicating good recyclability. Based on these results, CZIF-8/CNTs/CCBs could be used as an ideal material for efficient separation of oil–water mixtures, due to its superhydrophobic properties.

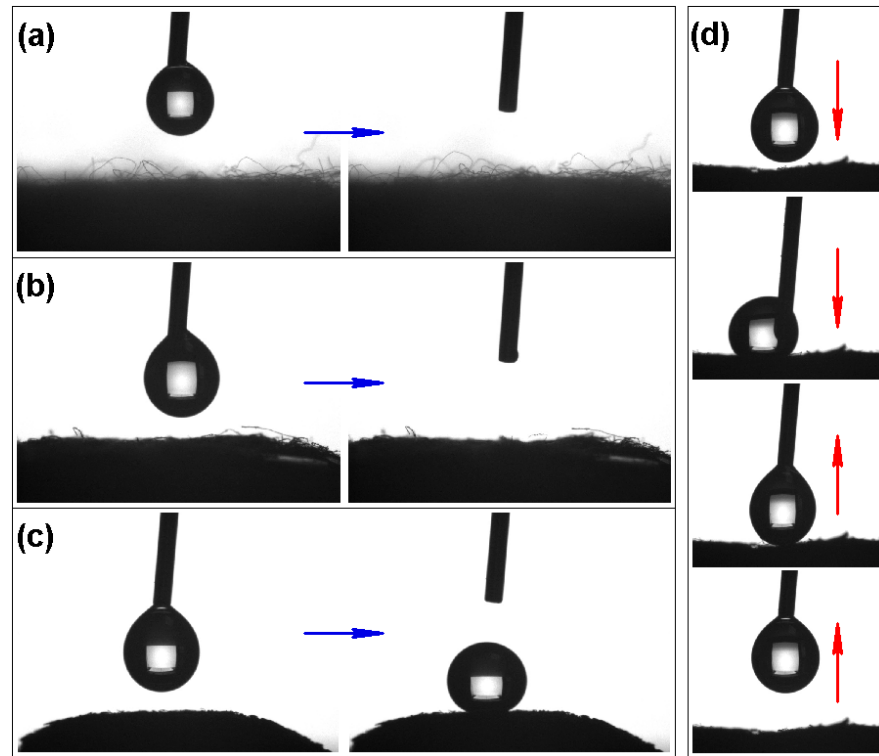


Figure 7. (a–c) The water static contact angle measurement for CBs, ZIF-8/CNTs/CBs, and CZIF-8/CNTs/CCBs. (d) Adhesion images of the water droplet on CZIF-8/CNTs/CCBs.

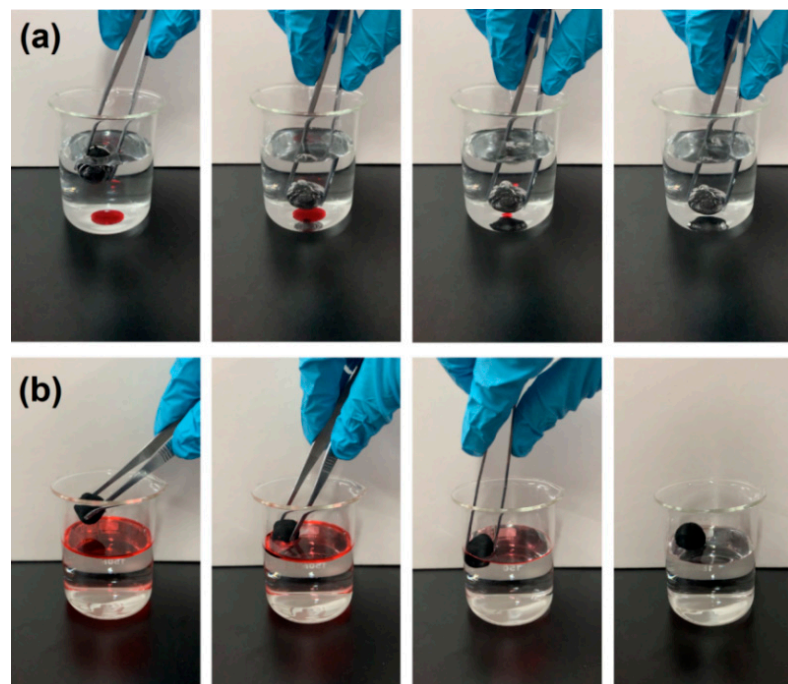
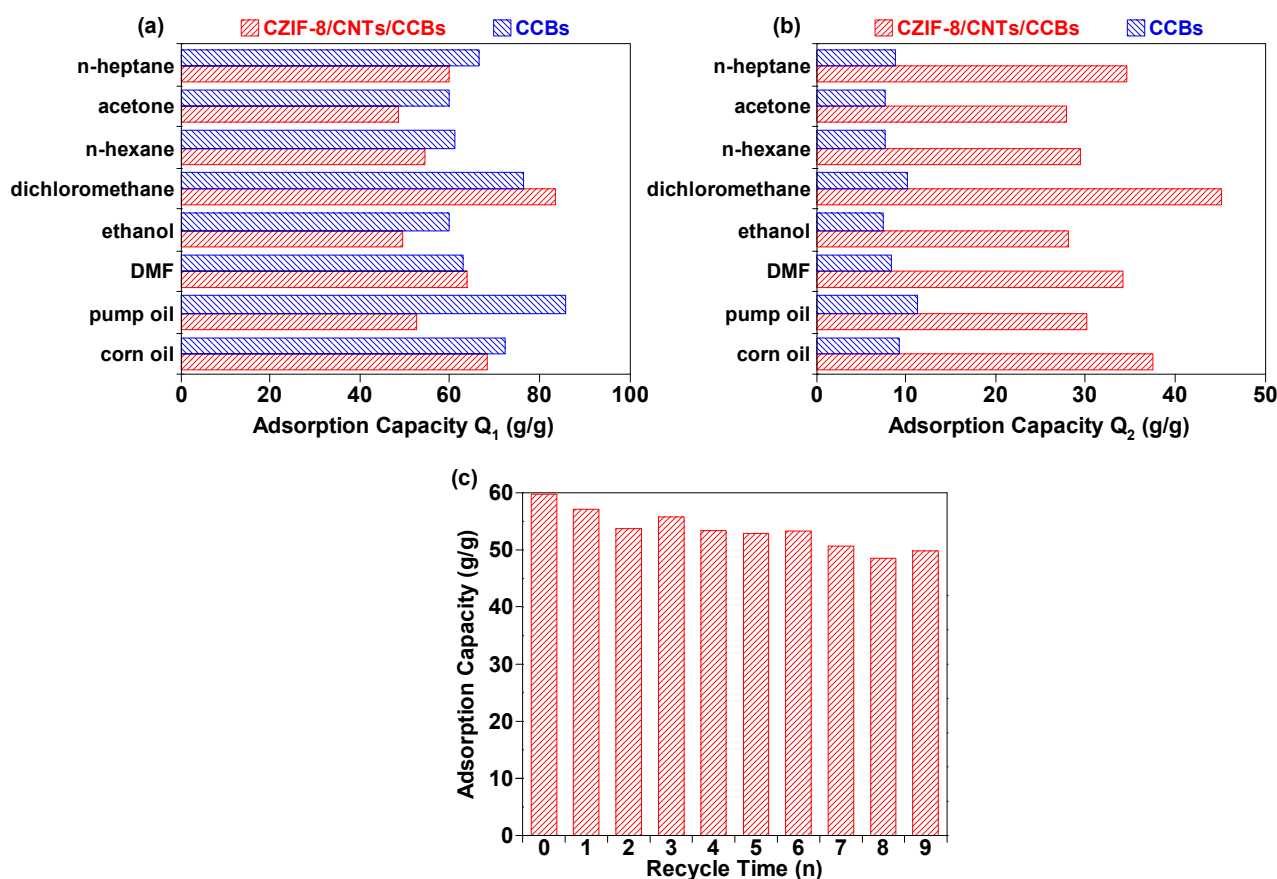


Figure 8. (a) Sorption process of dichloromethane (dyed with Oil Red O) by CZIF-8/CNTs/CCBs. (b) Sorption process of n-hexane (dyed with Oil Red O) by CZIF-8/CNTs/CCBs.



**Figure 9.** (a) Adsorption capacities  $Q_1$  of CZIF-8/CNTs/CCBs and CCBs for oil or organic solvents. (b) Adsorption capacities  $Q_2$  of CZIF-8/CNTs/CCBs and CCBs for oil or organic solvents. (c) Adsorption capacities of CZIF-8/CNTs/CCBs for n-heptane after 9 cycles.

**Table 1.** Comparison of various sorbent materials.

Sorbent Material	Absorbed Substances	Sorption Capacity (g.g <sup>-1</sup> )	Ref.
CNT/wood aerogel	oils and organic solvents	16–39	[39]
Silylated wood sponges	oils and organic solvents	17–41	[40]
Carbon nanotube sponges	oils	49–56	[41]
Polyvinyl-alcohol-reinforced wood sponge	oils and organic solvents	4–27	[42]
Microwrinkled reduced graphene oxide	oils	36–84	[43]
Cellulose-based aerogels	oils and organic solvents	45–99	[48]
Winter melon carbon aerogel	oils and organic solvents	16–50	[45]
Carbon nanofiber aerogel	oils and organic solvents	37–87	[46]
MOF-coated cotton fiber composite	oils and organic solvents	25–48	[31]
MOF-reduced graphene oxide aerogel	oils and organic solvents	45–147	[47]
Polyimide/MXene aerogels	oils and organic solvents	18–58	[44]
CZIF-8/CNTs/CCBs	oils and organic solvents	48–84	This work

#### 4. Conclusions

In summary, ZIF-8 and CNTs were fabricated in situ in the 3D interconnected network structure of CBs via a feasible strategy. Subsequently, carbonization treatment could effectively change the hydrophobic property of the sample. The characterization results suggested that CBs could be used as a porous structure for embedding ZIF-8 and CNTs, effectively improving the oil–water separation performance after carbonization. As an oleophilic and hydrophobic adsorbent, CZIF-8/CNTs/CCBs shows high sorption capacities of 48 to 84 times its own weight. Moreover, CZIF-8/CNTs/CCBs exhibits a stable oil

absorption capacity with reuse. This work provides a novel strategy for designing a superior adsorbent candidate for oil–water separation.

**Author Contributions:** Conceptualization, Y.S. and R.S.; methodology, Y.S.; validation, Z.K., C.S., and Q.W.; writing—original draft preparation, Y.S. and C.S.; writing—review and editing, Z.K., W.Y., and Z.Y. All authors have read and agreed to the published version of the manuscript.

**Funding:** This work was supported by Anhui Nature Science Research Program (KJHS2019B07), Anhui Provincial Nature Science Research Project (2008085MH269), Anhui Provincial Teaching Team Project (2020jxtD250), and Huangshan University Talent Introduction Funding (2018xkjQ005).

**Institutional Review Board Statement:** Not applicable.

**Informed Consent Statement:** Not applicable.

**Data Availability Statement:** Data sharing is not applicable.

**Conflicts of Interest:** The authors declare no conflict of interest.

## References

1. Yu, X.; Zhang, X.; Xing, Y.; Zhang, H.; Jiang, W.; Zhou, K.; Li, Y. Development of Janus Cellulose Acetate Fiber (CA) Membranes for Highly Efficient Oil-Water Separation. *Materials* **2021**, *14*, 5916. [[CrossRef](#)] [[PubMed](#)]
2. Sam, E.K.; Liu, J.; Lv, X. Surface Engineering Materials of Superhydrophobic Sponges for Oil/Water Separation: A Review. *Ind. Eng. Chem. Res.* **2021**, *60*, 2353–2364. [[CrossRef](#)]
3. Liu, H.; Geng, B.; Chen, Y.; Wang, H. Review on the Aerogel-Type Oil Sorbents Derived from Nanocellulose. *ACS Sustain. Chem. Eng.* **2016**, *5*, 49–66. [[CrossRef](#)]
4. Elhenawy, S.; Khraisheh, M.; AlMomani, F.; Hassan, M.K.; Al-Ghouti, M.A.; Selvaraj, R. Recent Developments and Advancements in Graphene-Based Technologies for Oil Spill Cleanup and Oil-Water Separation Processes. *Nanomaterials* **2021**, *12*, 87. [[CrossRef](#)]
5. Luo, W.; Sun, D.; Chen, S.; Shanmugam, L.; Xiang, Y.; Yang, J. Robust Microcapsules with Durable Superhydrophobicity and Superoleophilicity for Efficient Oil-Water Separation. *ACS Appl. Mater. Interfaces* **2020**, *12*, 57547–57559. [[CrossRef](#)]
6. Han, S.; Song, Q.; Feng, X.; Wang, J.; Zhang, X.; Zhang, Y. Flame-Retardant Silanized Boron Nitride Nanosheet-Infused Superhydrophobic Sponges for Oil/Water Separation. *ACS Appl. Nano Mater.* **2021**, *4*, 11809–11819. [[CrossRef](#)]
7. Kong, S.M.; Han, Y.; Won, N.I.; Na, Y.H. Polyurethane Sponge with a Modified Specific Surface for Repeatable Oil-Water Separation. *ACS Omega* **2021**, *6*, 33969–33975. [[CrossRef](#)]
8. Panickar, R.; Sobhan, C.B.; Chakravorti, S. Highly Efficient Amorphous Carbon Sphere-Based Superhydrophobic and Superoleophilic Sponges for Oil/Water Separation. *Langmuir* **2021**, *37*, 12501–12511. [[CrossRef](#)]
9. Wang, J.; Fan, Z.; Liu, Q.; Tong, Q.; Wang, B. Fabrication of PDMS@Fe<sub>3</sub>O<sub>4</sub>/MS Composite Materials and Its Application for Oil-Water Separation. *Materials* **2021**, *15*, 115. [[CrossRef](#)]
10. Ju, G.; Zhou, L.; Jiao, C.; Shen, J.; Luan, Y.; Zhao, X. One-Step Fabrication of a Functionally Integrated Device Based on Polydimethylsiloxane-Coated SiO<sub>2</sub> NPs for Efficient and Continuous Oil Absorption. *Materials* **2021**, *14*, 5998. [[CrossRef](#)]
11. Liu, D.; Wang, S.; Wu, T.; Li, Y. A Robust Superhydrophobic Polyurethane Sponge Loaded with Multi-Walled Carbon Nanotubes for Efficient and Selective Oil-Water Separation. *Nanomaterials* **2021**, *11*, 3344. [[CrossRef](#)] [[PubMed](#)]
12. Wu, F.; Pickett, K.; Panchal, A.; Liu, M.; Lvov, Y. Superhydrophobic Polyurethane Foam Coated with Polysiloxane-Modified Clay Nanotubes for Efficient and Recyclable Oil Absorption. *ACS Appl. Mater. Interfaces* **2019**, *11*, 25445–25456. [[CrossRef](#)] [[PubMed](#)]
13. Zhang, G.D.; Wu, Z.H.; Xia, Q.Q.; Qu, Y.X.; Pan, H.T.; Hu, W.J.; Zhao, L.; Cao, K.; Chen, E.Y.; Yuan, Z.; et al. Ultrafast Flame-Induced Pyrolysis of Poly(dimethylsiloxane) Foam Materials toward Exceptional Superhydrophobic Surfaces and Reliable Mechanical Robustness. *ACS Appl. Mater. Interfaces* **2021**, *13*, 23161–23172. [[CrossRef](#)] [[PubMed](#)]
14. Zhu, H.; Chen, D.; An, W.; Li, N.; Xu, Q.; Li, H.; He, J.; Lu, J. A Robust and Cost-Effective Superhydrophobic Graphene Foam for Efficient Oil and Organic Solvent Recovery. *Small* **2015**, *11*, 5222–5229. [[CrossRef](#)]
15. Bi, H.; Yin, Z.; Cao, X.; Xie, X.; Tan, C.; Huang, X.; Chen, B.; Chen, F.; Yang, Q.; Bu, X.; et al. Carbon fiber aerogel made from raw cotton: A novel, efficient and recyclable sorbent for oils and organic solvents. *Adv. Mater.* **2013**, *25*, 5916–5921. [[CrossRef](#)]
16. White, R.J.; Brun, N.; Budarin, V.L.; Clark, J.H.; Titirici, M.M. Always look on the “light” side of life: Sustainable carbon aerogels. *ChemSusChem* **2014**, *7*, 670–689. [[CrossRef](#)]
17. Yang, Y.; Tong, Z.; Ngai, T.; Wang, C. Nitrogen-rich and fire-resistant carbon aerogels for the removal of oil contaminants from water. *ACS Appl. Mater. Interfaces* **2014**, *6*, 6351–6360. [[CrossRef](#)]
18. Fu, C.; Gu, L.; Zeng, Z.; Xue, Q. One-Step Transformation of Metal Meshes to Robust Superhydrophobic and Superoleophilic Meshes for Highly Efficient Oil Spill Cleanup and Oil/Water Separation. *ACS Appl. Mater. Interfaces* **2020**, *12*, 1850–1857. [[CrossRef](#)]
19. Jiang, B.; Zhang, H.; Zhang, L.; Sun, Y.; Xu, L.; Sun, Z.; Gu, W.; Chen, Z.; Yang, H. Novel One-Step, In Situ Thermal Polymerization Fabrication of Robust Superhydrophobic Mesh for Efficient Oil/Water Separation. *Ind. Eng. Chem. Res.* **2017**, *56*, 11817–11826. [[CrossRef](#)]

20. Zhou, B.; Bashir, B.H.; Liu, Y.; Zhang, B. Facile Construction and Fabrication of a Superhydrophobic Copper Mesh for Ultraefficient Oil/Water Separation. *Ind. Eng. Chem. Res.* **2021**, *60*, 8139–8146. [[CrossRef](#)]
21. Lu, Z.; He, Y. Fabrication of superhydrophobic surfaces with tunable water droplet adhesion force by a two-step method. *Ceram. Int.* **2019**, *45*, 14389–14396. [[CrossRef](#)]
22. Kang, R.H.; Kim, D. Thermally Induced Silane Dehydrocoupling: Hydrophobic and Oleophilic Filter Paper Preparation for Water Separation and Removal from Organic Solvents. *Materials* **2021**, *14*, 5775. [[CrossRef](#)] [[PubMed](#)]
23. Kang, L.; Zhao, L.; Yao, S.; Duan, C. A new architecture of super-hydrophilic  $\beta$ -SiAlON/graphene oxide ceramic membrane for enhanced anti-fouling and separation of water/oil emulsion. *Ceram. Int.* **2019**, *45*, 16717–16721. [[CrossRef](#)]
24. Han, X.; Liu, S.; Shi, L.; Li, S.; Li, Y.; Wang, Y.; Chen, W.; Zhao, X.; Zhao, Y. ZIF-derived wrinkled Co<sub>3</sub>O<sub>4</sub> polyhedra supported on 3D macroporous carbon sponge for supercapacitor electrode. *Ceram. Int.* **2019**, *45*, 14634–14641. [[CrossRef](#)]
25. Si, Y.; Dong, Z.; Jiang, L. Bioinspired Designs of Superhydrophobic and Superhydrophilic Materials. *ACS Cent. Sci.* **2018**, *4*, 1102–1112. [[CrossRef](#)] [[PubMed](#)]
26. Silviana, S.; Darmawan, A.; Dalanta, F.; Subagio, A.; Hermawan, F.; Milen Santoso, H. Superhydrophobic Coating Derived from Geothermal Silica to Enhance Material Durability of Bamboo Using Hexadimethylsilazane (HMDS) and Trimethylchlorosilane (TMCS). *Materials* **2021**, *14*, 530. [[CrossRef](#)]
27. Tudu, B.K.; Sinhamahapatra, A.; Kumar, A. Surface Modification of Cotton Fabric Using TiO<sub>2</sub> Nanoparticles for Self-Cleaning, Oil-Water Separation, Antistain, Anti-Water Absorption, and Antibacterial Properties. *ACS Omega* **2020**, *5*, 7850–7860. [[CrossRef](#)]
28. Song, C.; Zhao, J.; Li, H.; Liu, L.; Li, X.; Huang, X.; Liu, H.; Yu, Y. One-Pot Synthesis and Combined Use of Modified Cotton Adsorbent and Flocculant for Purifying Dyeing Wastewater. *ACS Sustain. Chem. Eng.* **2018**, *6*, 6876–6888. [[CrossRef](#)]
29. Ferreira, V.C.; Wise, W.R.; Monteiro, O.C. Comparative study of powder and cotton-supported BiOCl particles on the photocatalytic degradation of industrial pollutants. *Ceram. Int.* **2020**, *46*, 27508–27516. [[CrossRef](#)]
30. Yang, L.; Zhan, Y.; Yu, R.; Lan, J.; Shang, J.; Dou, B.; Liu, H.; Zou, R.; Lin, S. Facile and Scalable Fabrication of Antibacterial CO<sub>2</sub>-Responsive Cotton for Ultrafast and Controllable Removal of Anionic Dyes. *ACS Appl. Mater. Interfaces* **2021**, *13*, 2694–2709. [[CrossRef](#)]
31. Dalapati, R.; Nandi, S.; Gogoi, C.; Shome, A.; Biswas, S. Metal-Organic Framework (MOF) Derived Recyclable, Superhydrophobic Composite of Cotton Fabrics for the Facile Removal of Oil Spills. *ACS Appl. Mater. Interfaces* **2021**, *13*, 8563–8573. [[CrossRef](#)] [[PubMed](#)]
32. Du, J.; Liu, L.; Hu, Z.; Yu, Y.; Zhang, Y.; Hou, S.; Chen, A. Raw-Cotton-Derived N-Doped Carbon Fiber Aerogel as an Efficient Electrode for Electrochemical Capacitors. *ACS Sustain. Chem. Eng.* **2018**, *6*, 4008–4015. [[CrossRef](#)]
33. Yue, Y.; Huang, Y.-L.; Bian, S.-W. Nitrogen-Doped Hierarchical Porous Carbon Films Derived from Metal–Organic Framework/Cotton Composite Fabrics as Freestanding Electrodes for Flexible Supercapacitors. *ACS Appl. Electron. Mater.* **2021**, *3*, 2178–2186. [[CrossRef](#)]
34. Singla, G.; Bhange, S.N.; Mahajan, M.; Kurungot, S. Facile synthesis of CNT interconnected PVP-ZIF-8 derived hierarchically porous Zn/N co-doped carbon frameworks for oxygen reduction. *Nanoscale* **2021**, *13*, 6248–6258. [[CrossRef](#)] [[PubMed](#)]
35. Wang, Y.; Zhang, N.; Tan, D.; Qi, Z.; Wu, C. Facile Synthesis of Enzyme-Embedded Metal-Organic Frameworks for Size-Selective Biocatalysis in Organic Solvent. *Front. Bioeng. Biotechnol.* **2020**, *8*, 714. [[CrossRef](#)] [[PubMed](#)]
36. Zhang, Y.; Jia, Y.; Li, M.; Hou, L. Influence of the 2-methylimidazole/zinc nitrate hexahydrate molar ratio on the synthesis of zeolitic imidazolate framework-8 crystals at room temperature. *Sci. Rep.* **2018**, *8*, 9597. [[CrossRef](#)]
37. Yin, W.; Li, M.; Hu, T.; Xue, Z.; Yu, J.; Chi, R. Preparation of an Adsorbent Based on Amidoxime and Triazole Modified Waste Cotton Fabrics through an Azide–Alkyne Click Reaction with Excellent Adsorption Performance toward Cu(II). *ACS Sustain. Chem. Eng.* **2018**, *7*, 1944–1955. [[CrossRef](#)]
38. Mu, J.; Shao, C.; Guo, Z.; Zhang, Z.; Zhang, M.; Zhang, P.; Chen, B.; Liu, Y. High photocatalytic activity of ZnO-carbon nanofiber heteroarchitectures. *ACS Appl. Mater. Interfaces* **2011**, *3*, 590–596. [[CrossRef](#)]
39. Zhu, Z.; Fu, S.; Lucia, L.A. A fiber-aligned thermal-managed wood-based superhydrophobic aerogel for efficient oil recovery. *ACS Sustain. Chem. Eng.* **2019**, *7*, 16428–16439. [[CrossRef](#)]
40. Guan, H.; Cheng, Z.; Wang, X. Highly compressible wood sponges with a spring-like lamellar structure as effective and reusable oil absorbents. *ACS Nano* **2018**, *12*, 10365–10373. [[CrossRef](#)]
41. Gui, X.; Zeng, Z.; Lin, Z.; Gan, Q.; Xiang, R.; Zhu, Y.; Cao, A.; Tang, Z. Magnetic and highly recyclable macroporous carbon nanotubes for spilled oil sorption and separation. *ACS Appl. Mater. Interfaces* **2013**, *5*, 5845–5850. [[CrossRef](#)] [[PubMed](#)]
42. Cai, Y.; Wu, Y.; Yang, F.; Gan, J.; Wang, Y.; Zhang, J. Wood sponge reinforced with polyvinyl alcohol for sustainable oil-water separation. *ACS Omega* **2021**, *6*, 12866–12876. [[CrossRef](#)]
43. Feng, C.; Yi, Z.; She, F.; Gao, W.; Peng, Z.; Garvey, C.J.; Dumeé, L.F.; Kong, L. Superhydrophobic and superoleophilic micro-wrinkled reduced graphene oxide as a highly portable and recyclable oil sorbent. *ACS Appl. Mater. Interfaces* **2016**, *8*, 9977–9985. [[CrossRef](#)] [[PubMed](#)]
44. Wang, N.N.; Wang, H.; Wang, Y.Y.; Wei, Y.H.; Si, J.Y.; Yuen, A.C.Y.; Xie, J.S.; Yu, B.; Zhu, S.E.; Lu, H.D.; et al. Robust, lightweight, hydrophobic, and fire-retarded polyimide/MXene aerogels for effective oil/water separation. *ACS Appl. Mater. Interfaces* **2019**, *11*, 40512–40523. [[CrossRef](#)] [[PubMed](#)]
45. Li, Y.-Q.; Samad, Y.A.; Polychronopoulou, K.; Alhassan, S.M.; Liao, K. Carbon aerogel from winter melon for highly efficient and recyclable oils and organic solvents absorption. *ACS Sustain. Chem. Eng.* **2014**, *2*, 1492–1497. [[CrossRef](#)]

46. Ieamviteevanich, P.; Palaporn, D.; Chanlek, N.; Poo-arporn, Y.; Mongkolthananaruk, W.; Eichhorn, S.J.; Pinitsoontorn, S. Carbon nanofiber aerogel/magnetic core-shell nanoparticle composites as recyclable oil sorbents. *ACS Appl. Nano Mater.* **2020**, *3*, 3939–3950. [[CrossRef](#)]
47. Sun, T.; Hao, S.; Fan, R.; Qin, M.; Chen, W.; Wang, P.; Yang, Y. Hydrophobicity-adjustable MOF constructs superhydrophobic MOF-rGO aerogel for efficient oil-water separation. *ACS Appl. Mater. Interfaces* **2020**, *12*, 56435–56444. [[CrossRef](#)]
48. Zhang, X.; Wang, H.; Cai, Z.; Yan, N.; Liu, M.; Yu, Y. Highly compressible and hydrophobic anisotropic aerogels for selective oil/organic solvent absorption. *ACS Sustain. Chem. Eng.* **2018**, *7*, 332–340. [[CrossRef](#)]